

REPORT DOCUMENTATION PAGE

Form Approved
OMB No. 0704-0188

The public reporting burden for this collection of information is estimated to average 1 hour per response, including the time for reviewing instructions, searching existing data sources, gathering and maintaining the data needed, and completing and reviewing the collection of information. Send comments regarding this burden estimate or any other aspect of this collection of information, including suggestions for reducing the burden, to Department of Defense, Washington Headquarters Services, Directorate for Information Operations and Reports (0704-0188), 1215 Jefferson Davis Highway, Suite 1204, Arlington, VA 22202-4302. Respondents should be aware that notwithstanding any other provision of law, no person shall be subject to any penalty for failing to comply with a collection of information if it does not display a currently valid OMB control number.

PLEASE DO NOT RETURN YOUR FORM TO THE ABOVE ADDRESS.

1. REPORT DATE (DD-MM-YYYY) 08-08-2007		2. REPORT TYPE Final report		3. DATES COVERED (From - To) June 1, 2003-May 31,2007	
4. TITLE AND SUBTITLE Enhancing the Interfacial and Dynamic Failure Behavior of Advanced Hybrid Structures Using Nanocomposite Materials				5a. CONTRACT NUMBER	
				5b. GRANT NUMBER N00014-03-1-0505	
				5c. PROGRAM ELEMENT NUMBER	
6. AUTHOR(S) Luoyu Roy Xu				5d. PROJECT NUMBER	
				5e. TASK NUMBER	
				5f. WORK UNIT NUMBER	
7. PERFORMING ORGANIZATION NAME(S) AND ADDRESS(ES) VANDERBILT UNIVERSITY DIVISION OF SPONSORED RESEARCH BAKER BUILDING SUITE 937 110 21ST AVENUE SOUTH				8. PERFORMING ORGANIZATION REPORT NUMBER	
9. SPONSORING/MONITORING AGENCY NAME(S) AND ADDRESS(ES) Office of Naval Research 100 Alabama St SW Suite 4R15 Atlanta, GA 30303-3104				10. SPONSOR/MONITOR'S ACRONYM(S)	
				11. SPONSOR/MONITOR'S REPORT NUMBER(S)	
12. DISTRIBUTION/AVAILABILITY STATEMENT Approved for Public Release; distribution is					
13. SUPPLEMENTARY NOTES					
14. ABSTRACT A novel interfacial joint was developed for reducing the interfacial stress levels. The proposed design, inspired by the shape and mechanics of trees, effectively removed the stress singularity at the interfacial joint for most engineering materials through an integrated theoretical and experimental investigation. Significant tensile loading capacity increase was obtained (up to 81%) using this new joint, while the material volume of the new joint actually was reduced. Dynamic tension experiments showed that the new convex joint yielded an increase in final failure strength (22%). This new joint can be employed to accurately evaluate the interfacial strength improvement of dissimilar material joints. Nanofiber-reinforced epoxy bonding with linker molecules was synthesized and tested for metal/metal and polymer/polymer joints. Mechanical properties including tension and shear bonding strengths showed very low increase or even decrease of nanocomposite bonding over that of pure epoxy bonding. Micromechanics analysis of nanocomposite materials revealed that the several factors for low proper increase were (a) finite end stress singularity of the discontinuous nanofiber and (b) low interfacial stress transfer of the nanofiber. In order to understand the failure mechanism of					
15. SUBJECT TERMS Nanocomposite Materials, Failure Mechanics, Interfacial Strength					
16. SECURITY CLASSIFICATION OF:			17. LIMITATION OF ABSTRACT UU	18. NUMBER OF PAGES 15	19a. NAME OF RESPONSIBLE PERSON L. R. Xu
a. REPORT U	b. ABSTRACT U	c. THIS PAGE U			19b. TELEPHONE NUMBER (Include area code) 615-343-4891

Project Information

Contract Number	N00014-03-1-0505 (Young Investigator Project)
Title of Research	Enhancing the Interfacial and Dynamic Failure Behavior of Advanced Hybrid Structures Using Nanocomposite Materials

L. Roy Xu*

Principal Investigator

Department of Civil and Environmental Engineering &
Interdisciplinary Materials Science Program
Vanderbilt University
Nashville, TN 37235

ONR 331 Program Director: Dr. Roshdy Barsoum

1. STATEMENT OF THE PROBLEM STUDIED

Composite structures will be the future naval ship structures to replace traditional steel structures, however, interfacial failure of composites/metal joints and sandwich structures is a major safety concern. This investigation is focused on solving new interface and failure mechanics problems, and developing nanocomposite materials as potential structural adhesives. Specially, our objectives are (1) developing novel interfacial joint designs for reducing the maximum interfacial stress level, and measuring intrinsic interfacial strengths of dissimilar material joints, and (2) evaluating static and dynamic response and failure behavior of hybrid joints using nanocomposite materials as structural adhesives. For objective (1), we employed a biologically inspired design. The proposed design, inspired by the shape and mechanics of trees, effectively removed the stress singularity at the interfacial joint for most engineering materials through an integrated theoretical and experimental investigation. For objective (2), we explored the fundamental understanding of toughening and failure mechanisms of nanocomposites using an integrated solid mechanics and material chemistry approach.

2. SUMMARY OF THE MOST IMPORTANT RESULTS

2.1 Interfacial and Failure Mechanics Areas

In the area of interfacial and failure mechanics, we have completed:

1. Systematic studies on the dynamic crack kinking at an interface. The purpose of this investigation is to identify major mechanics parameters in governing dynamic interfacial failure. The paper based on this investigation was published in *Engineering Fracture Mechanics*.

2. An analytical and experimental investigation on dynamic interfacial debonding ahead of a main crack. The purpose of this investigation is to control or suppress interface failure using mechanics and materials approaches. The paper based on this investigation was published in *International Journal of Solids and Structures*.
3. An analytical and numerical investigation on dynamic fracture of a metal plate bonded with different materials. The purpose of this investigation is to find major mechanics parameters in governing dynamic interfacial failure. The paper based on this investigation was published in *ASME Journal of Applied Mechanics*.
4. Systematic studies of the T-stress changes across static crack kinking. The purpose of this investigation is to control crack kinking (a common failure mode) using mechanics approaches. The paper based on this investigation was published in *ASME Journal of Applied Mechanics*.
5. An experimental and numerical investigation on adhesive bonding strengths of polymer materials. The purpose of this investigation is to provide an effective approach to measure bonding shear strengths. The paper based on this investigation was published in *International Journal of Adhesion and Adhesives*.
6. Design and tests of a biologically inspired design for dissimilar material joints with least free-edge stress singularities. The purpose of this investigation is to develop a novel approach to measure intrinsic interfacial tensile strengths for dissimilar materials and joints. The publications based on this investigation have been published in *Experimental Mechanics*.
7. Development of a convex dissimilar material joint with least free-edge stress singularities subjected to dynamic load. The purpose of this investigation is to evaluate the load capacity increase of the new dissimilar material joint. The publication based on this investigation was published in *Mechanics of Materials*.
8. Edge modifications for fiber pushout experiments of interfacial shear strength evaluation. The purpose of this investigation is to examine the shortcomings of the popular fiber pushout tests and propose a new test method. The publication based on this investigation was published in *Journal of Composite Materials*.

Theoretical background According to recent experimental and theoretical investigation, failure often occurs along the interfaces of dissimilar materials. Hence, reducing the interfacial stress level should improve structural safety and reliability. For our new interfacial joint design, we focused on the change of the stress singularity order λ , which is used in characterizing the asymptotic stress field of a bi-material corner (Bogy, 1971; Munz and Yang, 1993):

$$\sigma_{ij}(r, \theta) = \sum_{k=0}^N r^{-\lambda_k} K_k f_{ijk}(\theta) \quad (i, j = 1, 2, 3) \quad (1)$$

where $f_{ijk}(\theta)$ is an angular function and K_k is also called “stress intensity factor”. The theoretical stress values will become finite as r (defined in Figure 1(a)) approaches zero, if λ has a negative

real part. However, if λ has a positive real part, the interfacial stress level is always finite. Thus, we can eliminate the so-called “free-edge stress singularity”. We find it is possible to get such a value for λ as long as we vary two joint angles independently. Results of typical metal/polymer joints are shown in Figure 1(b). Such a design was inspired by the natural instinct observed in trees to grow in a convex manner, around a steel railing, that impedes the growth of the tree (Mattheck, 1998).

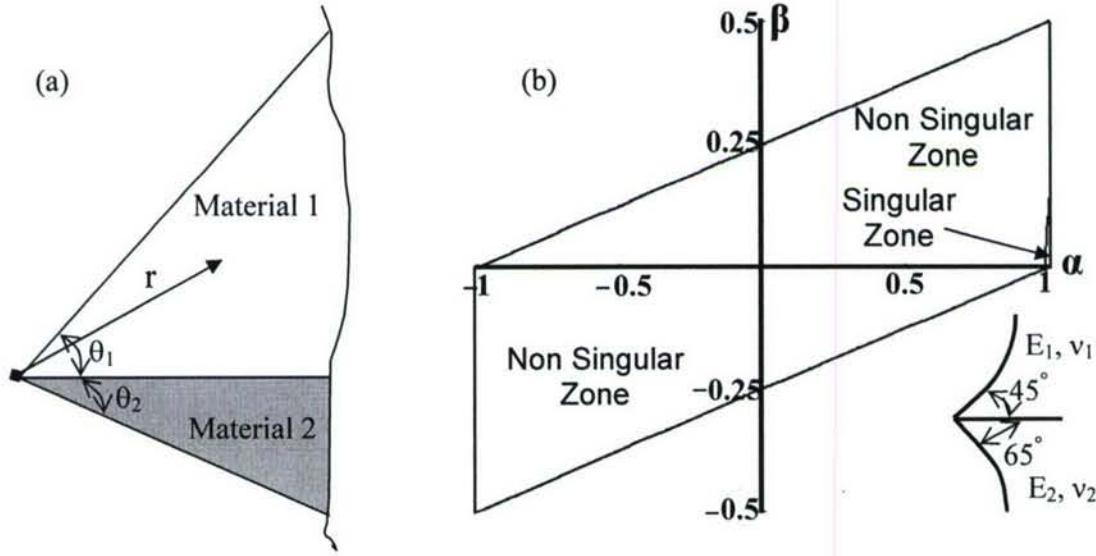


Fig.1(a). Angular definitions at bi-material corners or edges. (b) proposed convex joint could remove the free-edge stress singularity for most engineering combinations

New convex joints subjected to static and dynamic loading We find for a specific pair of interfacial joint angles of 65 and 45 degrees (Xu et al., 2004a), there is no stress singularity for most engineering material interfaces as shown in Figure 1(b). Generally, the material property mismatch is expressed in terms of the Dundurs' parameters α and β , which are two non-dimensional parameters computed from four elastic constants of two bonded materials:

$$\alpha = \frac{\mu_1 m_2 - \mu_2 m_1}{\mu_1 m_2 + \mu_2 m_1} \quad \beta = \frac{\mu_1 (m_2 - 2) - \mu_2 (m_1 - 2)}{\mu_1 m_2 + \mu_2 m_1} \quad (2)$$

where μ_1 is the shear modulus of material 1, μ_2 is the shear modulus of material 2, $m = 4(1 - \nu)$ for plane strain, ν is the Poisson's ratio and $m = 4/(1 + \nu)$ for plane stress (Dundurs, 1969). The photoelastic fringe concentrations caused by the free-edge stress singularity are clearly seen in our simulations and experiments in Figures 2(a), (b). Therefore, interfacial failure always initiates from the free edges of the traditional butt joints with straight edges. However, the stress singularity is successfully removed in our new convex joints as seen in Figure 2(c) using *in-situ* photoelasticity technique (Dally, 1979).

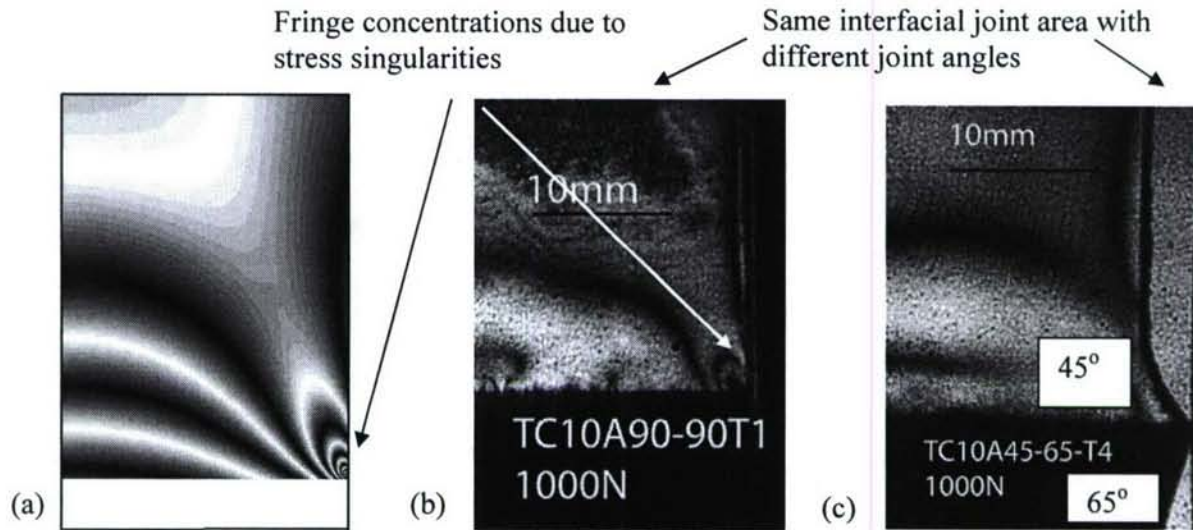


Fig. 2 (a), (b) Finite element simulations and *in-situ* photoelasticity experiments all showed high stress concentrations due to the free-edge stress singularity for a straight butt joint (c) No stress concentration was found in our proposed convex joints using *in-situ* photoelasticity

We designed and tested two types of dissimilar material joints (polymer/metal) as shown in Figure 3. Significant tensile loading capacity increase was obtained (up to 81%) in the proposed new joint while its material volume actually decreased by at least 15% over a traditional butt joint. The only payoff is around 10% increase in machining cost. Table 1 presents the measured nominal tensile strengths of two kinds of joints with different thicknesses.

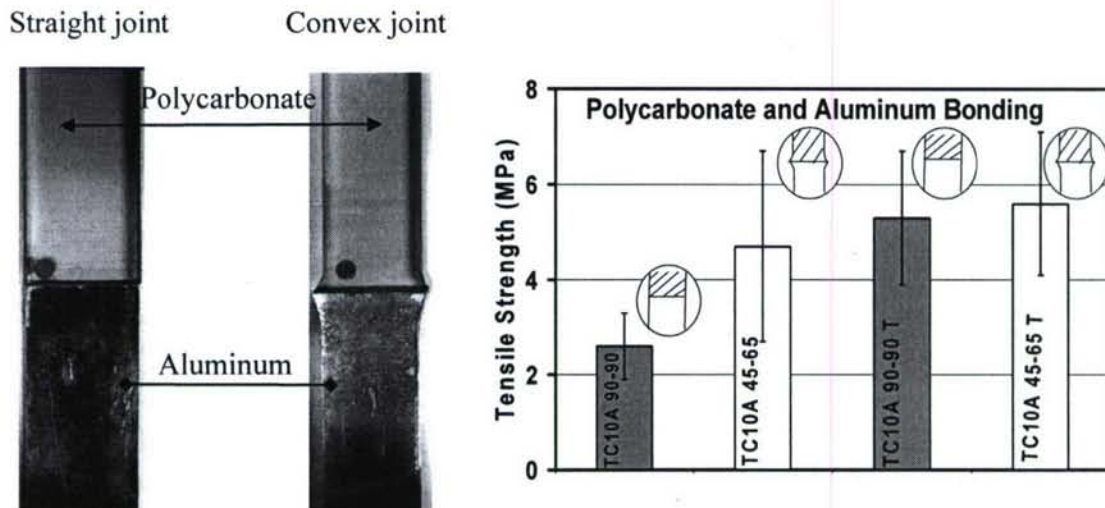


Fig. 3. Experimental data showing significant loading capacity increase (up to 81 %) in proposed new joints (right bar) over traditional butt joints (left bar-shadowed area).

Table 1. Tensile tests of polycarbonate-aluminum joints

Specimen code	Joint angles (PC-Al)	Tensile strength (MPa)	Change of strength	Standard deviation (MPa)	Specimen thickness (mm)
TC10A90-90	90- 90 (baseline)	2.6	0%	0.7	6
TC10A45-65	45-65	4.7	+81%	2.0	6
TC10A90-90T (thick specimens)	90-90 (baseline)	5.3	0%	1.4	9
TC10A45-65T (thick specimens)	45-65	5.6	+6%	1.5	9

However, in planar convex specimens, the free-edge stress singularity still exists at the straight free-edge along the thickness direction, although the stress singularity at the free-edge along the width direction is removed (Xu and Sengupta, 2004). Therefore, we further designed axisymmetric convex specimens, which completely removed free-edge stress singularities. The new joints were tested under dynamic tensile loading using a split Hopkinson tension bar (Wang and Xu, 2006). Significant tensile loading capacity increase was obtained (up to 22%) in new joints while the material volume of the new joints actually decreased by at least 18% over a traditional butt joint. Table 2 presents the measured nominal tensile strengths of two kinds of joints with different configurations.

Table 2. Dynamic tensile test data of aluminum/PMMA joints

Joint angles (metal-polymer)	Dynamic tensile strength (MPa)	Change of strength	Standard deviation (MPa)
90 ⁰ -90 ⁰ (baseline)	25.64	0%	4.77
65 ⁰ -45 ⁰	30.15	+17.59%	5.71

Improved interfacial shear strength measurements Meanwhile, we also tried to modify current shear bonding strength measurements. For similar materials joints such as PMMA bonded with PMMA, Iosipescu shear tests can be directly employed to measure shear bonding strengths (Xu et al., 2004c). For dissimilar material interface such as fiber/matrix interfaces in composite materials, the current fiber pushout/pullout tests are not reliable since significant stress free-edge stress singularities existed in these tests and other approaches such as micro-droplet tests should be used (Xu et al., 2005).

Fracture mechanics issues for interfacial failure The above investigation is focused on the perfect interfacial joint without any initial cracks or defects. However, in reality, there are cracks or defects in any joints. In order to further understand interfacial failure, transient response of a finite bimaterial plate with a crack perpendicular to and terminating at the interface (Figure 4) is analyzed for two types of boundaries (free-free and clamped-clamped). The crack surface is

loaded by arbitrary time-dependent antiplane shear impact. The mixed initial-boundary value problem is reduced to a singular integral equation of a generalized Cauchy kernel for the crack tearing displacement density or screw dislocation density. The Gauss-Jacobi quadrature technique is employed to numerically solve the singular integral equation, and then the dynamic stress intensity factors are determined by implementing a numerical inversion of the Laplace transform (Li and Xu, 2006). As an example, numerical calculations are carried out for a cracked bimaterial plate composed of aluminum (material I) and epoxy or steel (material II). The effects of material properties, geometry, and boundary types on the variations of dynamic stress intensity factors are discussed. Results indicate that an overshoot of the normalized stress intensity factor of the crack tip at the interface decreases for a cracked bimaterial plate, and the occurrence of which is delayed for a cracked aluminum/epoxy plate compared to a pure aluminum plate with the same crack.

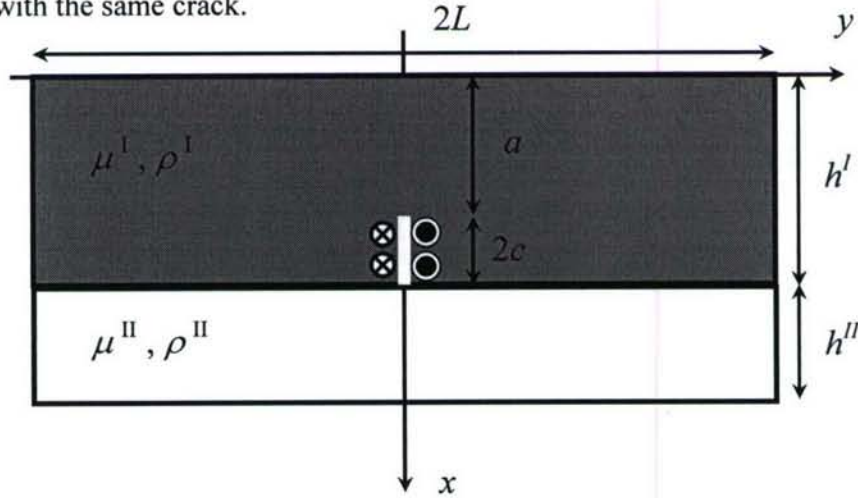


Fig. 4. A finite bimaterial plate with a through crack perpendicular to and terminating at the interface.

Meanwhile, we have systematically explored the possible crack kink (often occurs at interfaces) to determine the necessary T-stress formats. The change of the T-stresses before and after crack kinking and its relation with the crack growth stability is highlighted (Li and Xu, 2007). For an open main crack, there is only one T-stress term along the main crack in the rectangular coordinate system. This T-stress before crack kinking could be decomposed into three terms based on a possible kink direction, i.e. (1) normal T-stress along the kinking path, $T_{rr} = T \cos^2 \theta$ (2) normal T-stress perpendicular to the kinking path, $T_{\theta\theta} = T \sin^2 \theta$ (3) shear T-stress along the kinking path, $T_{r\theta} = -T \cos \theta \sin \theta$. These three terms make different contribution to the mechanics parameters of the kinked crack. If the kinked crack is open, the normal T-stress perpendicular to the kinking path before crack kinking affects the mode-I stress intensity factor of the kinked crack; the shear T-stress along the kinking path contributes to the mode-II stress intensity factor of the kinked crack; while the T-stress of the kinked crack only has one term for a two dimensional solid. The T-stress for an open kink is a function of the kinked crack length and the stress intensity factors of the main crack, and is different from the T-stress before crack kinking. If the kinked crack is closed, i.e. its mode-I stress intensity factor is zero, then two T-stress terms for the kinked crack are necessary, which are contributed by the (1) normal T-stress along the kinking path, (2) normal T-stress perpendicular to the kinking path

before crack kinking. Of course, the shear T-stress along the kinking path before crack kinking still contributes to the mode-II stress intensity factor of the kinked crack. Therefore, it is easily understood that the T-stress formats of a closed main crack with two possible kink types. There are also two non-singular T-stresses for the closed main crack. For an open kink, only one T-stress term and two stress intensity factors are involved while for a closed kink, two T-stress terms and one stress intensity factor are important from mechanics viewpoint. These results are very helpful to analyze a crack kinking along a material interface. It is also noticed that since the sign of the T-stress of a kinked open crack might be different from that of a main crack as seen in Figure 5, simply using the sign of the T-stress before crack kinking is not sufficient to determine crack growth stability as observed in recent experiments.

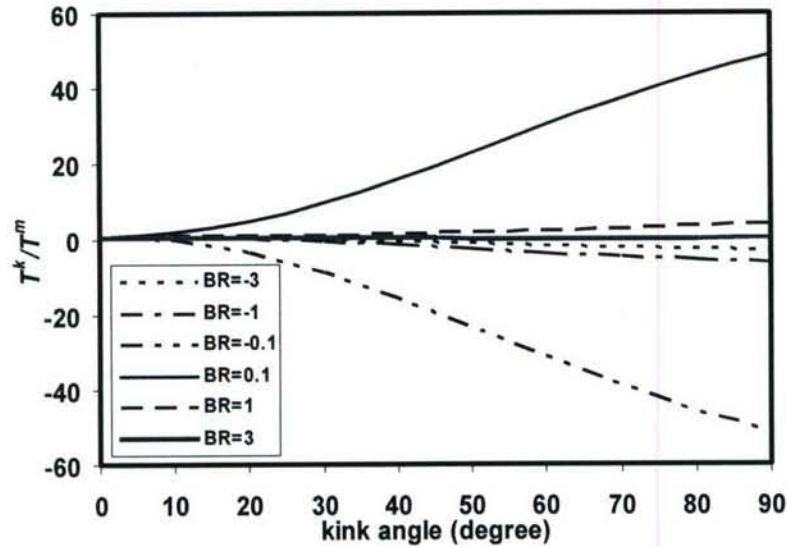


Fig. 5. T-stress variations of the kinked crack and main crack T^k/T^m with biaxial ratio BR and kink angle for $2a/l=100$

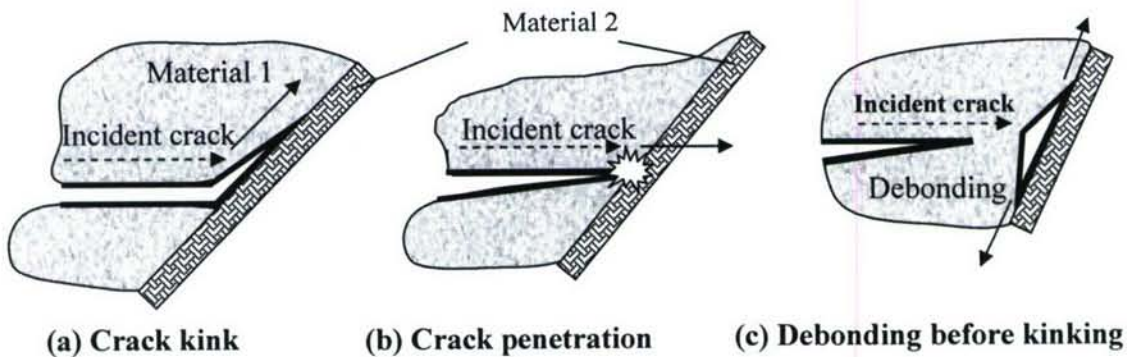


Fig. 6. Common failure modes when a crack encounters an interface.

In order to understand the failure mechanism of nanocomposite materials, or other dissimilar material joints, new failure criteria are much needed for modeling and simulations. When a crack propagates in an elastic solid and encounters an interface, one of the three situations may occur as seen in Figure 6: (a) after the crack reaches the interface, it kinks out of its original path

and continues to propagate along the interface. This phenomenon is often called “crack kinking or deflection” (Xu and Wang, 2006); (b) the crack penetrates the interface and continues to propagate along its original path, i.e., crack penetration; (c) early interface debonding initiates before the incident crack reaches the interface, or it refers to the “Cook-Gordon mechanism” (Cook and Gordon, 1964). In the open literature, efforts have been primarily focused on analyzing the first two cases, crack kinking and crack penetration (Hutchinson and Suo, 1992; Gupta et al., 1992; Arata et al., 2000). The objective in this investigation is to understand the mechanics and material insight of interfacial debonding initiation induced by a dynamic incident mode-I crack as seen in Figure 6(c). In order to avoid complicated stress waves across a bimaterial interface, and to simplify dynamic fracture mechanics modeling, two kinds of bonded brittle polymers were used to conduct dynamic fracture experiments. Meanwhile, dynamic fracture mechanics modeling incorporating an interfacial strength criterion was developed to predict interfacial debonding initiation and compared with experimental observations.

A strength criterion was used to predict the interfacial crack initiation (Xu and Wang, 2006b):

$$\left(\frac{\sigma'_{22}}{\sigma_t}\right)^2 + \left(\frac{\sigma'_{12}}{\sigma_s}\right)^2 = 1 \quad (3)$$

where σ_t, σ_s are the tensile and shear strengths of the interface. $\sigma_{11}, \sigma_{12}, \sigma_{22}$ are stress components of a steady crack tip in the main coordinate system and $\sigma'_{11}, \sigma'_{12}, \sigma'_{22}$ are stresses acting on the interface which are obtained by stress tensor transformation. The stress field of a steady dynamic crack is a function of combined time and length scales (Freund, 1990):

$$\sigma_{ij}(t, r, \theta, V) = \frac{K_I(t)}{\sqrt{2\pi r}} \sum_{ij}^I(\theta, V) + T\delta_{i1}\delta_{j1} + \frac{K_{II}(t)}{\sqrt{2\pi r}} \sum_{ij}^{II}(\theta, V) + O(r) \quad (i, j = 1, 2) \quad (4)$$

Combining equations (3) and (4), the critical distance r_c (the horizontal distance from the main crack tip to the interfacial crack initiation location) can be predicted. Then, we can systemically investigate how to suppress the interfacial debonding. Obviously, the interfacial strength is an important parameter to govern interfacial debonding initiation based on our proposed criteria. To clarify the interfacial strength effect on the interfacial debonding initiation, and to examine which interfacial strength is more critical, variations of the critical distances with the interfacial tensile and shear strengths are shown in Figure 7. Obviously, with the increase of the interfacial tensile or shear strength, the critical distance decreases. Moreover, as shown in Figure 7(a), the critical distance decreases sharply with the increase of the interfacial tensile strength. However, different shear strength values do not lead to much difference in the critical distances as seen in Figure 7(b). Therefore, the interfacial tensile strength is much more important than the interfacial shear strength to control interfacial debonding initiation in this case (a mode-I incident crack). Although the above results are based on bonded polymer systems, they are expected to be extended to bimaterial systems. For example, high stress intensity factors of the incident cracks and low interfacial tensile strengths will easily induce early interfacial debonding in bimaterial systems.

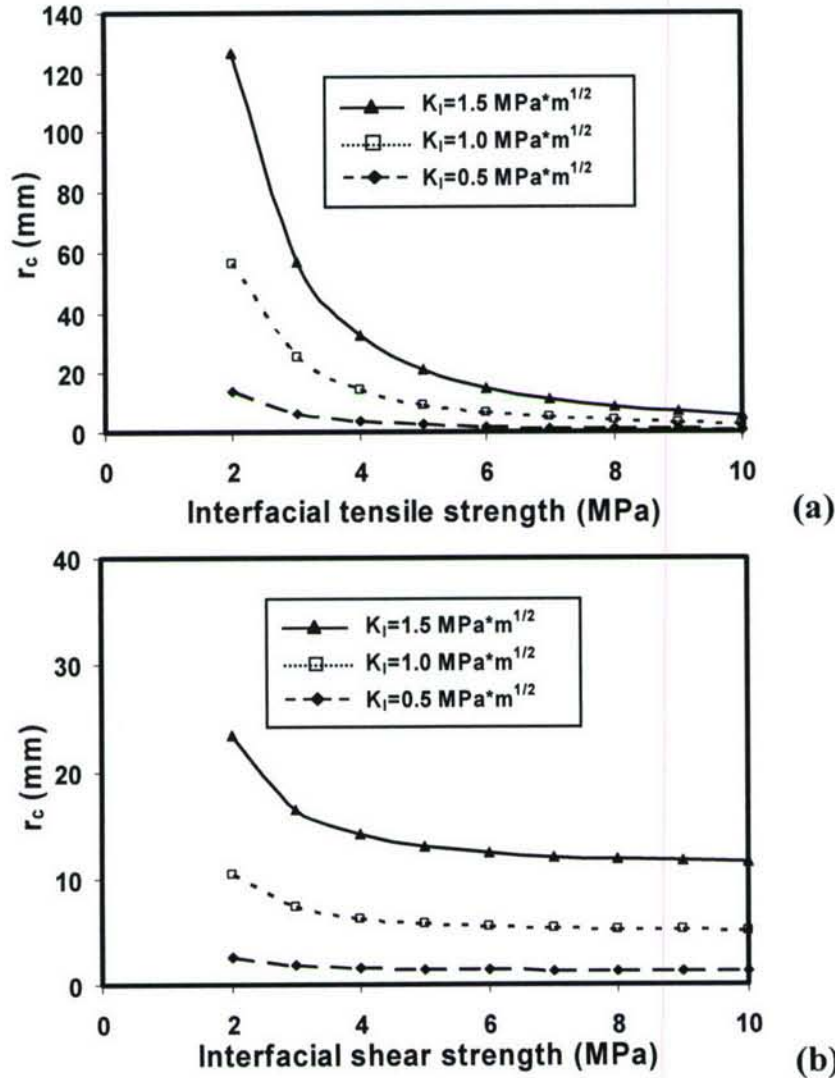


Fig.7, Variations of the critical distance r_c with (a) interfacial tensile strength (fixed shear strength $\tau_s = 7.47 \text{ MPa}$); and (b) interfacial shear strength (fixed tensile strength $\sigma_t = 6.75 \text{ MPa}$) for different stress intensity factors under the conditions of $V/C_s = 0.4$, $\beta = 30^\circ$, $T = 0 \text{ MPa}$.

Meanwhile, dynamic fracture mechanics theory was employed to analyze the crack deflection behavior of dynamic mode-I cracks propagating towards inclined weak planes/interfaces in otherwise homogenous elastic solids. When the incident mode I crack reached the weak interface, it kinked out of its original plane and continued to propagate along the weak interface. The dynamic stress intensity factors and the nonsingular T stresses of the incident cracks were fitted, and then dynamic fracture mechanics concepts were used to obtain the stress intensity factors of the kinked cracks as functions of kinking angles and crack tip speeds. The T-stress of the incident crack has a small positive value but the crack path was quite stable. In order to validate fracture mechanics predictions, the theoretical photoelasticity fringe patterns of the

kinked cracks were compared with the recorded experimental fringes. Moreover, the mode-mixity of the kinked crack was found to depend on the kinking angle and the crack tip speed. A weak interface will lead to a high mode-II component and a fast crack tip speed of the kinked mixed-mode crack.

2.2 Nanocomposite Material Area

In the area of nanocomposite materials, we have completed:

1. Mechanical property characterization of a polymeric nanocomposite reinforced by graphitic nanofibers with reactive linkers (Xu et al., 2004b). The purpose of this investigation is to examine complete mechanical properties using bulk specimens of nanocomposites. The publication based on this investigation was published in *Journal of Composite Materials*. **(Top 5 in 2005; and top 10 in 2006 of the Most-Frequently-Read Articles in *Journal of Composite Materials*)**
2. Interfacial stress transfer and property mismatch analyses in discontinuous nanocomposite materials. The purpose of this investigation is to seek mechanics insight of low strength improvement of discontinuous nanocomposite materials. The publication based on this investigation was published by *Journal of Nanoscience and Nanotechnology* (Xu and Sengupta, 2005).
3. Mechanical property characterization of nanocomposite adhesives reinforced by graphitic nanofibers. The publication based on this investigation was published in *Journal of Nanoscience and Nanotechnology* (Xu et al. 2007).

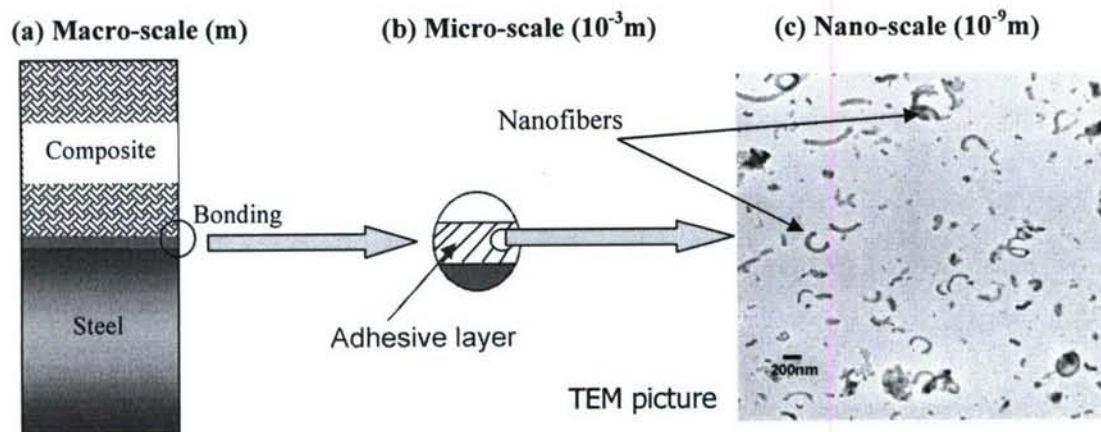


Fig. 8(a), (b). Nanocomposite bonding applied to a hybrid joint (c). Transmission Electron Microscope (TEM) image of nanofibers as uniformly dispersed in epoxy

We developed so-called “nanocomposite bonding” to increase bonding strengths as illustrated in Figure 8(a). In nanocomposite materials, at least the length-scale in one direction of the reinforcement should be in the range of nano-meters. So far, we have synthesized and tested nanofiber/epoxy composites through collaboration with Prof. C. M. Lukehart’s group of the Chemistry Department at Vanderbilt University. Strong and tough nanofibers were prepared as

crystalline graphite fibers having average diameters as small as 25 nm and having atomic structures such that edge carbon atom surface sites are present along the entire length of the carbon nanofiber. Chemical modification of these surface carbon sites and subsequent reaction with bifunctional linker molecules provides surface-derivatized nanofibers that can covalently bind to polymer resin molecules. By ensuring that a high number density of surface sites on each nanofiber forms covalent bonds to polymer resin molecules, a carbon nanofiber/polymer interface of high covalent binding integrity can be achieved. A TEM micrograph shows that nanofibers have excellent dispersion (Xu et al., 2004b).

Due to the rapid rate and low temperature required for adhesive resin curing, we invested certain processing conditions to ensure high-quality bonding. In order to simplify the mechanics problems, our nanofiber-reinforced epoxy is only used in similar material joints, i.e., aluminum/aluminum bonds and PMMA/PMMA bonds. As shown in Figure 9, shear bonding strengths of PMMA/PMMA bonds of different nanofiber-reinforced adhesives with various fiber percents and processing conditions sometimes increased, but sometimes decreased too. Similar results were also observed for tensile bonding strengths (Xu et al., 2007). Overall, we find that current nanocomposite materials cannot significantly improve bonding strengths.

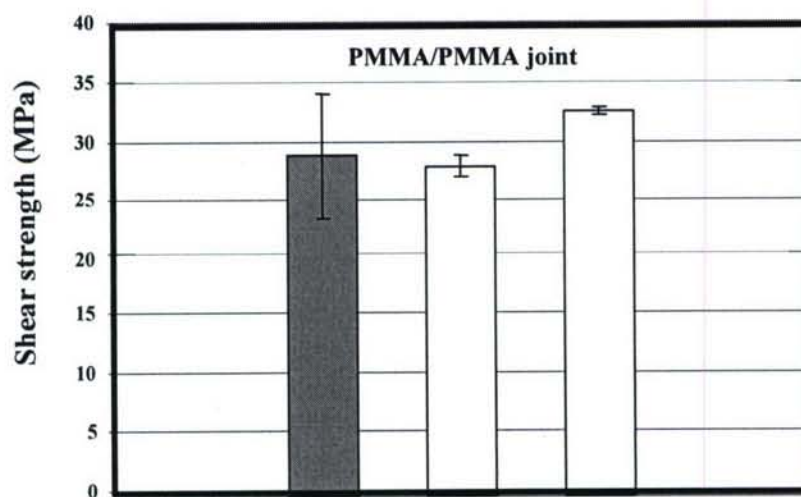


Fig. 9. Shear strength comparisons of various PMMA/PMMA bonds featuring nanofiber-reinforced composites with different fiber weight percents and processing conditions (left bar—pure epoxy bonding)

Indeed, a similar trend of low increase or uncertain data pertaining to nanocomposite bonding was also observed in bulk specimens, as shown in Figure 10. Three-point-bending experiments of pure epoxy and nanofiber-reinforced epoxy specimens recorded some increase in fracture toughness for one composite system and some decrease in another composite system (Xu et al., 2004b). Overall, we cannot draw a conclusion that current nanocomposite materials will significantly improve strengths or fracture toughnesses of the matrix materials. In order to design better nanocomposite materials, we explored this phenomenon using an approach based on micromechanics of composite materials.

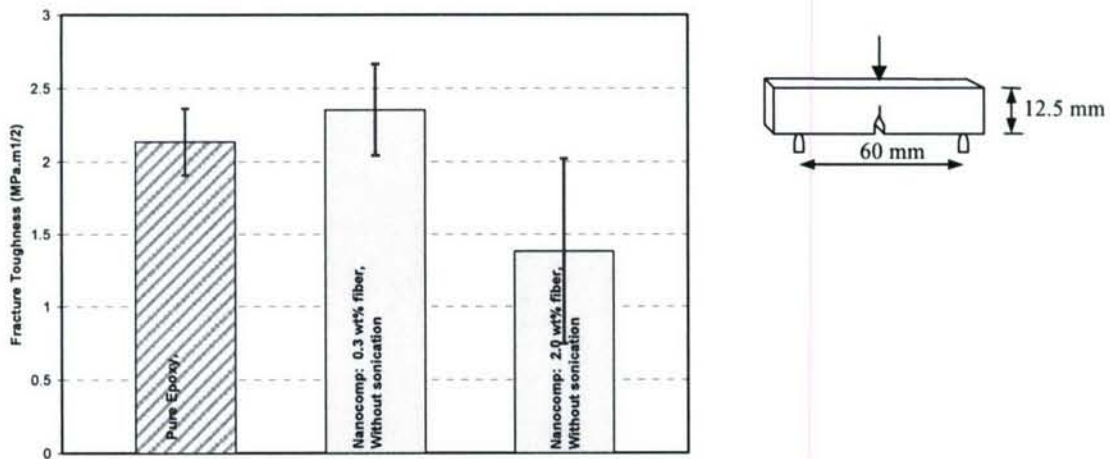


Fig. 10. Experimental data show that nanocomposites may decrease or increase the fracture toughnesses.

We investigated the interfacial stress transfer and possible stress singularities arising at the finite ends of discontinuous nanofibers embedded in a matrix (Xu and Sengupta, 2005). Round-ended nanofibers were also proposed to remove the interfacial singular stresses, which were caused by stiffness mismatch of the very stiff nanofiber and the soft matrix. However, the normal stress along the loading direction in the nanofiber through interfacial stress transfer was still less than two times that in the matrix. This is far below the high strength capability of the nanofiber as shown in Figure 11. Hence, nanofibers or nanotubes in continuous forms, which preclude the formation of singular interfacial stress zones, are recommended over discontinuous nanofibers to achieve high strengths in future nanocomposite materials.

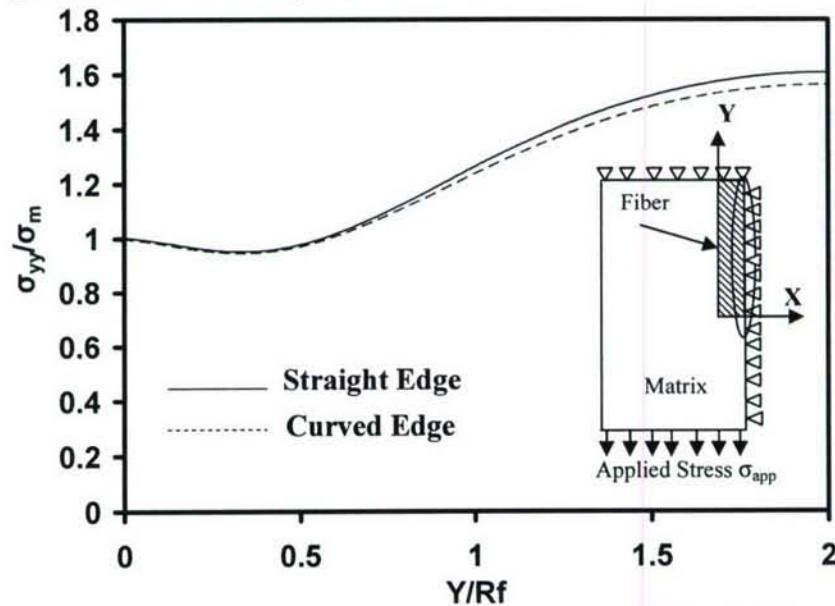


Fig.11. Normal stress distribution comparison in a nano-fiber inside nanocomposite materials subjected to tensile load (stress value is based on the fiber mid-section). For straight edged and round edged nanofiber

3. BIBLIOGRAPHY

- Arata, J.J.M., Needleman, A., Kumar, K.S., and Curtin, W.A., 2000. Microcrack nucleation and growth in lamellar solids. *International Journal of Fracture*, 105, 321-342.
- Bogy, D.B., 1971. Two edge-bonded elastic wedges of different materials and wedge angles under surface tractions. *Journal of Applied Mechanics*, 38, 377-386.
- Cook, J., and Gordon, J.E., 1964. A mechanism for the control of crack propagation in all brittle systems. *Proceedings of the Royal Society of London*, 282A, 508-520.
- Dally, J.W., 1979. Dynamic photoelastic studies of fracture. *Experimental Mechanics*, 19, 349-361.
- Dundurs, J., 1969. Discussion of edge-bonded dissimilar orthogonal elastic wedges under normal and shear loading by Bogy D.B.. *ASME, Journal of Applied Mechanics*, 36, 650-652.
- Freund, L.B., 1990. *Dynamic Fracture Mechanics*. Cambridge University Press, New York.
- Gupta, V., Argon, A.S., and Suo, Z., 1992. Crack deflection at an interface between two orthotropic materials. *Journal of Applied Mechanics*, 59, s79-s87.
- Hutchinson, J.W., and Suo, Z., 1992. Mixed mode cracking in layered materials. *Advances in Applied Mechanics*, 29, 63-191.
- Mattheck, C., 1998. *Design in Nature: Learning from Trees*, Springer-Verlag, New York.
- Munz, D., and Yang, Y.Y., 1993. Stresses near the edge of bonded dissimilar materials described by two stress intensity factors. *International Journal of Fracture*, 60, 169-177.
- Li, X.F., and L. R. Xu, 2006 Transient Response of a Finite Bimaterial Plate Containing a Crack Perpendicular to and Terminating at the Interface, *ASME Journal of Applied Mechanics*,
- Wang, P. and L. R. Xu, 2006. Convex Interfacial Joints with Least Stress Singularities In Dissimilar Materials and Structures, *Mechanics of Materials*, 2006, Vol.38, pp.1001-1011.2006,Vol.73, pp.544-554.
- Li, X.F., and L. R. Xu, 2007. T-stresses across Static Crack Kinking, *ASME Journal of Applied Mechanics*, 2007, Vol. 74, Vol. 181-190.
- Xu, L. R., and S. Sengupta, 2004. Dissimilar Material Joints with and without Free-edge Stress Singularities; Part II: An Integrated Numerical Analysis, *Experimental Mechanics*, 2004, Vol. 44, pp. 616-621.
- Xu, L. R. H. Kuai and S. Sengupta, 2004a. Dissimilar Material Joints with and without Free-edge Stress Singularities; Part I: A Biologically Inspired Design, *Experimental Mechanics*, 2004, Vol. 44, pp. 608-615.

Xu, L. R., V. Bhamidipati, W.-H. Zhong, Ji. Li, C. M. Lukehart, E. Lara-Curzio, K. C. Liu and M. J. Lance, 2004b. Mechanical Property Characterization of A Polymeric Nanocomposite Reinforced by Graphitic Nanofibers with Reactive Linkers,” *Journal of Composite Materials*, 2004, Vol. 38, pp.1563-1582

Xu, L. R., S. Sengupta and H. Kuai, 2004c An Experimental and Numerical Investigation on Adhesive Bonding Strengths of Polymer Materials, *International Journal of Adhesion and Adhesives*, 2004, Vol. 24, pp. 455–460.

Xu, L. R., H. Kuai* and S. Sengupta, 2005. Free-Edge Stress Singularities and Edge Modifications for Fiber Pushout Experiments, *Journal of Composite Materials*, 2005, Vol. 39, pp.1103-1125.

Xu, L. R. and S. Sengupta, 2005. Interfacial Stress Transfer and Property Mismatch in Discontinuous Nanofiber/nanotube Composite Materials, *Journal of Nanoscience and Nanotechnology*, 2005, Vol. 5, pp.620-626.

Xu, L. R. and P. Wang, 2006b. Dynamic Interfacial Debonding Initiation Induced by An Incident Crack, *International Journal of Solids and Structures*, 2006, Vol. 43, pp.6535-6550.

Xu, L. R. and P. Wang, 2006a Dynamic Fracture Mechanics Analysis of Failure Mode Transitions along Weaken Interfaces in Elastic Solids, *Engineering Fracture Mechanics*, 2006, Vol. 73, 1597-1614.

Xu, L. R., L. Li, C. M. Lukehart and H. Kuai, 2007, Mechanical Property Characterization Nanofiber-Reinforced Composite Adhesives, *Journal of Nanoscience and Nanotechnology*, 2007, Vol. 7, pp.1-3.

4. Appendixes—List of journal papers citing ONR support (*---graduate student)

1. L. R. Xu, L. Li, C. M. Lukehart and H. Kuai*, 2007, "Mechanical Property Characterization Nanofiber-Reinforced Composite Adhesives," *Journal of Nanoscience and Nanotechnology*, Vol. 7, pp.1-3.
2. X.F. Li, and L. R. Xu, 2007. "T-stresses across Static Crack Kinking," *ASME Journal of Applied Mechanics*, 2007, Vol. 74, Vol. 181-190.
3. L. R. Xu and P. Wang*, 2006a. "Dynamic Interfacial Debonding Initiation Induced by An Incident Crack," *International Journal of Solids and Structures*, 2006, Vol. 43, pp.6535-6550.
4. P. Wang* and L. R. Xu, 2006. "Convex Interfacial Joints with Least Stress Singularities In Dissimilar Materials and Structures," *Mechanics of Materials*, 2006, Vol.38, pp.1001-1011.
5. X.F. Li, and L. R. Xu, 2006 "Transient Response of a Finite Bimaterial Plate Containing a Crack Perpendicular to and Terminating at the Interface," *ASME Journal of Applied Mechanics*, 2006, Vol.73, pp.544-554.
6. L. R. Xu and P. Wang*, 2006b "Dynamic Fracture Mechanics Analysis of Failure Mode Transitions along Weaken Interfaces in Elastic Solids," *Engineering Fracture Mechanics*, 2006, Vol. 73, 1597-1614.
7. L. R. Xu, H. Kuai* and S. Sengupta*, 2005. "Free-Edge Stress Singularities and Edge Modifications for Fiber Pushout Experiments," *Journal of Composite Materials*, 2005, Vol. 39, pp.1103-1125.
8. L. R. Xu and S. Sengupta*, 2005. "Interfacial Stress Transfer and Property Mismatch in Discontinuous Nanofiber/nanotube Composite Materials," *Journal of Nanoscience and Nanotechnology*, 2005, Vol. 5, pp.620-626.
9. L. R. Xu, and S. Sengupta*, 2004. "Dissimilar Material Joints with and without Free-edge Stress Singularities; Part II: An Integrated Numerical Analysis," *Experimental Mechanics*, 2004, Vol. 44, pp. 616-621.
10. L. R. Xu, H. Kuai* and S. Sengupta*, 2004a. "Dissimilar Material Joints with and without Free-edge Stress Singularities; Part I: A Biologically Inspired Design," *Experimental Mechanics*, 2004, Vol. 44, pp. 608-615.
11. L. R. Xu, V. Bhamidipati *, W.-H. Zhong, Ji. Li, C. M. Lukehart, E. Lara-Curzio, K. C. Liu and M. J. Lance, 2004b. "Mechanical Property Characterization of A Polymeric Nanocomposite Reinforced by Graphitic Nanofibers with Reactive Linkers," *Journal of Composite Materials*, 2004, Vol. 38, pp.1563-1582 (**Top 5 in 2005; and top 10 in 2006 of the Most-Frequently-Read Articles in Journal of Composite Materials**)
12. L. R. Xu, S. Sengupta* and H. Kuai*, 2004c "An Experimental and Numerical Investigation on Adhesive Bonding Strengths of Polymer Materials," *International Journal of Adhesion and Adhesives*, 2004, Vol. 24, pp. 455-460.